Pergamon

Int. J. Heat Mass Transfer. Vol. 39, No. 8, pp. 1639–1647, 1996

0017–9310/96 $15.00+0.00

0017–9310(95)00258–8

Convection and stability in a rotating porous layer with alternating direction of the centrifugal body force

P. VADASZ

Department of Mechanical Engineering, University of Durban-Westville,
Private Bag X54001, Durban 4000, South Africa

(*Received* 10 *March* 1995 *and in final form* 28 *June* 1995)

Abstract—An alternating direction of the centrifugal body force results when the axis of rotation is placed within the boundaries of a rotating fluid saturated porous layer. The onset of thermal convection and stability in a fluid saturated porous layer prevailing such conditions is investigated analytically. The marginal stability criterion was evaluated in terms of a critical centrifugal Rayleigh number and a corresponding critical wave number. The effect of the offset distance of the layer's cold wall from the axis of rotation on the convection is analyzed, showing that the critical centrifugal Rayleigh and wave numbers increase significantly as the layer's cold wall moves away from the rotation axis. This leads eventually to unconditional stability when the layer's hot wall coincides with the rotation axis. This unconditional stability prevails when the axis of rotation moves away from the porous domain, so that the imposed temperature gradient opposes the direction of the centrifugal acceleration. Significant effects on the convection pattern are identified as a result of the rotation axis location.

1. INTRODUCTION

The problem of convection and stability in rotating porous media has a focal interest following theoretical, as well as practical, relevance of transport phenomena in rotating porous media to applications in engineering and geophysics [1, 2]. *Gravity* driven convection in rotating porous media was investigated [3–7] for a single fluid or binary mixture. The *centrifugal acceleration* as a driving body force in generating free convection was considered by Vadasz [1] to present a three-dimensional solution for the case when the temperature gradient, resulting from the imposed conditions on the boundary, is perpendicular to the centrifugal body force. The solution focused on the effect of the Coriolis force on the basic free convection for high values of Ekman number. When the temperature gradient resulting from the imposed boundary conditions is collinear with the centrifugal body force, a stability problem is to be formulated. Vadasz [8] presented the solution to this stability problem for porous layers *adjacent to the axis of rotation*. The corresponding stability analysis and solution for a porous layer placed *an arbitrary positive distance from the center of rotation* was presented by Vadasz [9], where a singularity in the solution associated with negative values of the offset distance from the axis of rotation was identified. It is this resulting singularity and its consequences which forms the objective of the present investigation. As this occurs at *negative values of the offset distance from the axis of rotation* it implies that the location of the rotation axis falls within the boundaries of the porous domain (or to the left side of the cold wall—a case of little interest due to its inherent unconditional stability). This particular location of the rotation axis causes positive values of the centrifugal acceleration on the right side of the rotation axis and negative values on its left side. The objective of the investigation is to establish the stability condition, i.e. the critical centrifugal Rayleigh number, the critical wave number and the corresponding eigenfunctions for different locations of the axis of rotation within the boundaries of the porous domain.

2. PROBLEM FORMULATION

A narrow fluid saturated porous layer subject to rotation is placed such that the axis of rotation lies within the boundaries of the fluid domain. The layer is heated on the right wall, cooled on the left wall and the remaining walls are insulated. The cold wall is therefore placed a dimensionless distance x_0 from the center of rotation as presented in Fig. 1. The offset distance is presented in a dimensionless form representing the ratio between the dimensional offset distance and the length of the porous layer in the form $x_0 = x_{0*}/L_*$. Two systems of coordinates are presented in Fig. 1, the first (x', y', z') is linked to the axis of rotation and the second (x, y, z), placed a horizontal distance x_0 apart from the first one, belongs to the

NOMENCLATURE

H	the front aspect ratio of the porous layer, equals H_*/L_*
W	the top aspect ratio of the porous layer, equals W_*/L_*
$\hat{\mathbf{e}}_x$	unit vector in the x direction
$\hat{\mathbf{e}}_y$	unit vector in the y direction
$\hat{\mathbf{e}}_z$	unit vector in the z direction
$\hat{\mathbf{e}}_n$	unit vector normal to the boundary, positive outwards
H_*	the height of the layer
k_*	permeability of the porous domain
L_*	the length of the porous layer
M_f	a ratio between the heat capacity of the fluid and the effective heat capacity of the porous domain
M	the rank of the Galerkin approximation
p	reduced pressure generalized to include the constant component of the centrifugal term (dimensionless)
$\mathbf{q}$	dimensionless filtration velocity vector, equals $u\hat{\mathbf{e}}_x+v\hat{\mathbf{e}}_y+w\hat{\mathbf{e}}_z$
Ra_ω	porous media centrifugal Rayleigh number related to the contribution of the horizontal location within the porous layer to the centrifugal acceleration, equals $\beta_*\Delta T_c\omega^2{}_*L_*^2k_*M_f/\alpha_{e*}\nu_*$
R	scaled centrifugal Rayleigh number, equals Ra_ω/π^2
T	dimensionless temperature, equals $(T_*-T_C)/(T_H-T_C)$
T_C	coldest wall temperature
T_H	hottest wall temperature
u	horizontal x component of the filtration velocity
v	horizontal y component of the filtration velocity
w	vertical component of the filtration velocity
W_*	the width of the layer
x_0	the dimensionless offset distance from the rotation center, equals x_{0*}/L_*
x	horizontal length coordinate, in the layer's system of coordinates
y	horizontal width coordinate, in the layer's system of coordinates
z	vertical coordinate, in the layer's system of coordinates
x'	horizontal length coordinate, linked to the rotation axis system of coordinates
y'	horizontal width coordinate, linked to the rotation axis system of coordinates
z'	vertical coordinate, linked to the rotation axis system of coordinates.

Greek symbols

α	a parameter related to the wave number, equals κ^2/π^2
α_{e*}	effective thermal diffusivity.
β	a parameter, equals $(1/2-\lvert x_0\rvert)$
β_*	thermal expansion coefficient
γ^2	a parameter, equals $256/81\pi^4$
δ_{ij}	Kronecker delta function
ϕ	porosity
ω_*	angular velocity of the rotating box
ν_*	fluid's kinematic viscosity
κ	wave number
μ_*	fluid's dynamic viscosity
ψ	stream function
ΔT_c	characteristic temperature difference.

Subscripts

*	dimensional values
c	characteristic values
cr	critical values
C	related to the coldest wall
H	related to the hottest wall
t	transition value.

porous layer coordinates. As the axis of rotation lies within the boundaries of the porous domain the value of x_0 is not positive. It is therefore convenient to introduce this fact into the problem formulation, specifying explicitly that $x_0 = -|x_0|$. A positive temperature gradient in the x-direction is anticipated as a result of the imposed thermal boundary conditions. The centrifugal acceleration is collinear with the temperature gradient, however, its direction alternates depending on the location within the porous layer. At the right of the rotation axis the centrifugal acceleration is positive, while at its left it becomes negative.

The front aspect ratio of the layer is defined as $H = H_*/L_*$ where H_* and L_* are the height and the length of the layer, respectively. The top aspect ratio is $W = W_*/L_*$, where W_* is the width of the layer. The following analysis is confined to a narrow layer, i.e. $W \ll 1$. Free convection may occur as a result of the centrifugal body force while the gravity force is neglected. The only inertial effect considered is the centrifugal acceleration, as far as changes in density are concerned. Other than that, the Darcy's law is assumed to govern the fluid flow (extended to include the centrifugal acceleration), while the Boussinesq

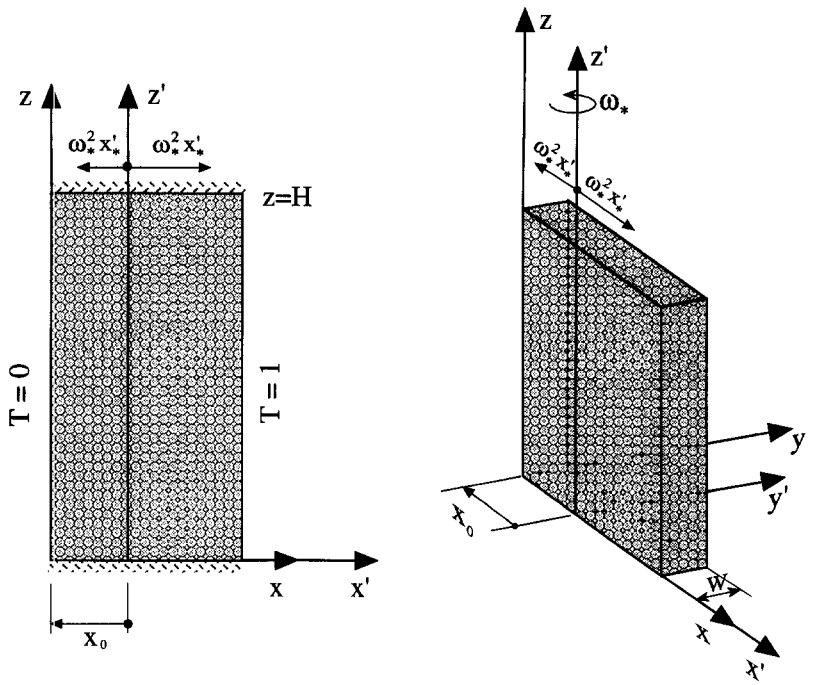

Fig. 1. A rotating fluid saturated porous layer having the rotation axis within its boundaries and subject to different temperatures at the sidewalls.

approximation is applied for the effects of density variations. As a narrow layer is considered, i.e. $W \ll 1$, a Cartesian coordinate system can be used and the component of the centrifugal acceleration in the y direction can be neglected. Under these conditions the following dimensionless set of governing equations is obtained:

$$\nabla \cdot \mathbf{q} = 0 \tag{1}$$

$$\mathbf{q} = -\nabla p - Ra_\omega [x - |x_0|] T \hat{\mathbf{e}}_x \tag{2}$$

$$\frac{\partial T}{\partial t} + \mathbf{q} \cdot \nabla T = \nabla^2 T. \tag{3}$$

Equations (1)–(3) are presented in a dimensionless form. The values $\alpha_{e*}/L_* M_f$, $\mu_* \alpha_{e*}/k_* M_f$, and $\Delta T_c = (T_H - T_C)$ are used to scale the filtration velocity components (u_*, v_*, w_*), pressure (p_*), and temperature variations $(T_* - T_C)$, respectively, where α_{e*} is the effective thermal diffusivity, μ_* is the fluid's viscosity, k_* is the permeability of the porous matrix and M_f is the ratio between the heat capacity of the fluid and the effective heat capacity of the porous domain. The length of the layer L_* was used for scaling the variables x_*, y_* and z_*. Accordingly, $x = x_*/L_*$, $y = y_*/L_*$ and $z = z_*/L_*$. In equation (2) one observes the centrifugal Rayleigh number defined by

$$Ra_\omega = \beta_* \Delta T_c \omega_*^2 L_*^2 k_* M_f / \alpha_{e*} v_*.$$

An additional controlling parameter appears in the equations representing the offset distance from the center of rotation, i.e. $|x_0|$.

As all the boundaries are rigid the solution must follow the impermeability conditions there, i.e. $\mathbf{q} \cdot \hat{\mathbf{e}}_n = 0$ on the boundaries, where $\hat{\mathbf{e}}_n$ is a unit vector normal to the boundary. The temperature boundary conditions are: $T = 0$ at $x = 0$, $T = 1$ at $x = 1$ and $\nabla T \cdot \hat{\mathbf{e}}_n = 0$ on all other walls representing the insulation condition on these walls.

The partial differential equations (1)–(3) form a nonlinear coupled system which, together with the corresponding boundary conditions, accepts a basic motionless conduction solution. The establishment of the conditions of stability of this basic solution is the objective of this analysis.

3. METHOD OF SOLUTION

A basic motionless solution in the form

$$\mathbf{q}_b = 0 \quad T_b = x$$

$$p_b = -Ra_\omega [|x_0| x^2/2 + x^3/3] + \text{const.} \tag{4}$$

satisfies the governing equations an the boundary conditions. Therefore the solution is presented as the sum of this *basic solution* and *small perturbations* in the form

$$\mathbf{q} = \mathbf{q}_b + \mathbf{q}' \quad T = T_b + T' \quad p = p_b + p', \tag{5}$$

where the (′) stands for perturbed values. Substituting

equations (4) and (5) into the governing equations (1)–(3), and linearizing the result by neglecting terms which include products of perturbations which are small, yields the following set of linear partial differential equations for the perturbations

$$\nabla \cdot \mathbf{q}' = 0 \tag{6}$$

$$\mathbf{q}' = -\nabla p' - Ra_\omega[x-|x_0|]T'\hat{\mathbf{e}}_x \tag{7}$$

$$\left[\frac{\partial}{\partial t}-\nabla^2\right]T'+u' = 0. \tag{8}$$

Applying twice the *curl* operator on equation (7) and using the property of $\mathbf{q}'$ being a solenoidal vector which comes out from equation (6), eliminates the pressure from the system of equations (6)–(8). The remaining coupling between the temperature and filtration velocity perturbations in the resulting equations can be resolved, leading to one equation for the temperature perturbations in the form

$$\left[\left(\frac{\partial}{\partial t}-\nabla^2\right)\nabla^2 - Ra_\omega(x-|x_0|)\left(\frac{\partial^2}{\partial y^2}+\frac{\partial^2}{\partial z^2}\right)\right]T' = 0. \tag{9}$$

Assuming an expansion into normal modes in the y and z directions, i.e. $T' = A_\kappa\theta(x)\,e^{\sigma t+i(\kappa_y y+\kappa_z z)}$ yields the following ordinary differential equation for θ

$$[(D^2-\kappa^2-\sigma)(D^2-\kappa^2)-Ra_\omega(x-|x_0|)\kappa^2]\theta = 0, \tag{10}$$

where $D \equiv \mathrm{d}/\mathrm{d}x$, $\kappa^2 = \kappa_y^2+\kappa_z^2$ and κ_y, κ_z are the wave numbers in the y and z directions, respectively.

The Galerkin method is adopted to solve equation (10). Consequently $\theta(x)$ is expanded in a series of orthogonal trial functions $\phi_m(x)$ which satisfy the boundary conditions in the form

$$\theta(x) = \sum_{m=1}^{M} a_m\phi_m(x). \tag{11}$$

The principle of exchange of stabilities holds for this problem and at marginal stability $\sigma = 0$. Upon substitution of expansion (11) into equation (10), one can multiply the resulting equation by $\phi_i(x)$ and integrate over the length of the domain to obtain

$$\sum_{m=1}^{M} a_m\left[\int_0^1 \phi_i(D^4-2\kappa^2D^2)\phi_m\,\mathrm{d}x + (\kappa^4+Ra_\omega|x_0|\kappa^2)\int_0^1 \phi_m\phi_i\,\mathrm{d}x - Ra_\omega\kappa^2\int_0^1 x\phi_m\phi_i\,\mathrm{d}x\right] = 0. \tag{12}$$

In the particular case considered here, the choice $\phi_m = \sin(m\pi x)$ proved to be a trial function which satisfies the necessary conditions. Upon substitution of this trial function into equation (12) and performing the integrals, a homogeneous set of linear algebraic equations is obtained in the form

$$\sum_{m=1}^{M}\left[[(m^2+\alpha)^2-\alpha\beta R]\frac{\delta_{mi}}{2} + \frac{4R\alpha mi}{(m^2-i^2)^2\pi^2}\delta_{m+i,2p-1}\right]a_m = 0 \tag{13}$$

for $i = 1, 2, 3, \ldots, M$, where the following scaling and notation was introduced for convenience

$$R = \frac{Ra_\omega}{\pi^2} \quad \alpha = \frac{\kappa^2}{\pi^2} \quad \beta = (\tfrac{1}{2}-|x_0|). \tag{14}$$

In equation (13) δ_{ij} is the Kronecker delta function and the index p can take arbitrary integer values; it stands only for setting the second index in the Kronecker delta function to be an odd integer. Equation (13) has the form $\mathbb{L}(a_m) = 0$, representing a homogeneous linear system accepting a non-zero solution only for particular values of R such that $\det[\mathbb{L}(a_m)] = 0$.

4. RESULTS AND DISCUSSION

Although the research on these values of R and more particularly on the critical ones, has been done by solving (13) up to the rank $M = 11$ for different values of $|x_0|$, useful information can be drawn by considering the approximation to rank $M = 2$. For this rank of approximation the system reduces to two equations which are expressed in the following matrix representation:

$$\begin{bmatrix}((1+\alpha)^2-\alpha\beta R)/2; & 8R\alpha/9\pi^2 \\ 8R\alpha/9\pi^2; & ((4+\alpha)^2-R\alpha\beta)/2\end{bmatrix}\begin{bmatrix}a_1\\a_2\end{bmatrix} = 0. \tag{15}$$

Taking the determinant of equation (15) and equating it to zero leads to the characteristic values of R in the form

$$R_c = \frac{\beta[(1+\alpha)^2+(4+\alpha)^2]\pm\sqrt{\beta^2[(1+\alpha)^2+(4+\alpha)^2]^2-4(\beta^2-\gamma^2)(1+\alpha)^2(4+\alpha)^2}}{2\alpha(\beta^2-\gamma^2)}, \tag{16}$$

where $\gamma^2 = 256/81\pi^4$. A singularity is observed in equation (16) when $\beta^2 = \gamma^2$. This singularity corresponds to $\beta = \gamma$ or $\beta = -\gamma$. Since β is uniquely related to the offset distance $|x_0|$ and $\gamma = 16/9\pi^2$ is a constant, one can relate the singularity to specific values of $|x_0|$, namely $|x_0| = (9\pi^2 - 32)/18\pi^2 = 0.3199$ and $|x_0| = (9\pi^2 + 32)/18\pi^2 = 0.680$. The first value $|x_0| = 0.3199$, corresponds to the transition from two positive roots of equation (16) for R_c when $|x_0| < 0.3199$, to one positive root and one negative root of equation (16) for R_c, when $|x_0| > 0.3199$. This transition is of no significant consequence to the establishment of the stability criterion. The second value of $|x_0| = 0.680$, corresponds to the transition from one positive root and one negative root of equation (16) for R_c, when $0.3199 < |x_0| < 0.68$, to two negative roots for R_c, when $|x_0| > 0.68$. Therefore the second transition has significant consequences in establishing the stability condition, as for $|x_0| \geqslant 0.68$ no positive roots R_c of equation (16) exist. This implies an unconditional stability of the basic solution (4) (i.e. all modes of perturbations decay) for all values of R if $|x_0| \geqslant 0.68$. This transition value of $|x_0|$ was investigated at higher ranks leading to $|x_0| \geqslant 0.765$ at rank $M = 3$. At any rank M an Mth order algebraic equation is obtained by equating the determinant of the linear system $\mathbb{L}(a_m) = 0$ (given by equation (13)) to zero, in the form

$$c_M R^M + c_{M-1} R^{M-1} + \cdots + c_3 R^3 + c_2 R^2 + c_1 R + c_0 = 0. \quad (17)$$

The transition value of $|x_0|$ was found to correspond to the condition causing the reduction of the order of equation (17) by one, i.e. to $c_M = 0$. Accordingly, the transition values $|x_0|$ for different ranks were evaluated and are presented in Table 1. From the table it can be observed that the transition value of $|x_0|$ associated with the existence of unconditional stability, increases with increasing the rank. It is clearly established that unconditional stability exists for $|x_0| \geqslant 1$, as this represents the case when the imposed temperature gradient opposes the direction of the centrifugal acceleration for all values of x within the domain. Although the existence of a smaller transition value of $|x_0|$ causing unconditional stability was not definitely excluded, the indications are that as the rank increases, the transition value of $|x_0|$ tends towards the limit value of 1.

The characteristic curves of $Ra_{\omega,c}$ as a function of κ were established at rank $M = 11$ by using *Mathematica*™ [10] for symbolic as well as numerical computations. The results in terms of Ra_ω/π^2 as a function of

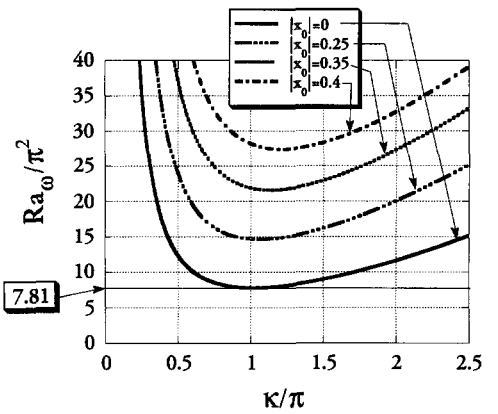

Fig. 2. The characteristic curves representing the marginal stability limit for different values of $|x_0|$.

κ/π for values of $|x_0|$ varying between $|x_0| = 0$ and $|x_0| = 0.4$ are presented in Fig. 2. For $|x_0| = 0$ the critical value of $Ra_{\omega,cr} = 7.81\pi^2$, as presented by Vadasz [8], was reconfirmed. The results for R_{cr} vs $|x_0|$ are presented in Fig. 3 in order to observe the effect of $|x_0|$ on the critical values of Ra_ω. A significant increase in the critical values of Ra_ω as $|x_0|$ approaches the limit value of 1, is observed from Fig. 3. A logarithmic scale was used in Fig. 3a to present the results of R_{cr} over the whole range of values $|x_0| \in [0, 1]$, while a linear scale is used in Fig. 3b to present R_{cr} over the limited range of $|x_0| \in [0, 0.5]$. The critical wave number increases significantly as $|x_0|$ increases, particularly for values of $|x_0|$ higher than 0.4, as can be observed from Fig. 4. This means that convection cells become shorter in the z direction if the aspect ratio is maintained constant as $|x_0|$ increases.

Once the critical values of Ra_ω and κ are evaluated, the results can be used to calculate the ratio between the coefficients in the series equation (11). Since the linear stability does not allow for the evaluation of the amplitude of convection, the coefficient a_1 can be absorbed into the definition of the amplitude A_κ, therefore leaving in the series the ratios $b_m = a_m/a_1$ $\forall\, m = 1, 2, \ldots, M$, where $b_1 = 1$ by definition. Evaluating the coefficients, b_m, up to rank $M = 11$ for different $|x_0|$ values becomes essentially the problem of finding an eigenvector belonging to the system $\mathbb{L}(a_m) = 0$ and corresponding to the singular operator $\mathbb{L}$. This means that the required eigenvector is associated with a zero eigenvalue of the operator $\mathbb{L}$. This procedure was applied by using *Mathematica*™ [10]. Insignificant discrepancies between the values of b_m at different ranks were identified for values of $|x_0|$ below 0.5. However, as $|x_0|$ increased beyond 0.5 significant

Table 1. Transition values of $|x_0|$ for different ranks of M

M	2	3	4	5	6	7	8	9	10	11
$\lvert x_0\rvert_t$	0.680	0.765	0.815	0.847	0.8695	0.886	0.899	0.9097	0.918	0.925

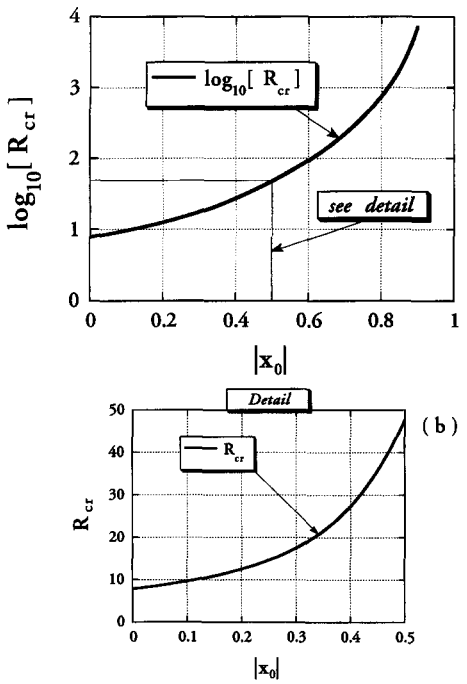

Fig. 3. The variation of the critical values of the centrifugal Rayleigh number as a function $|x_0|$.

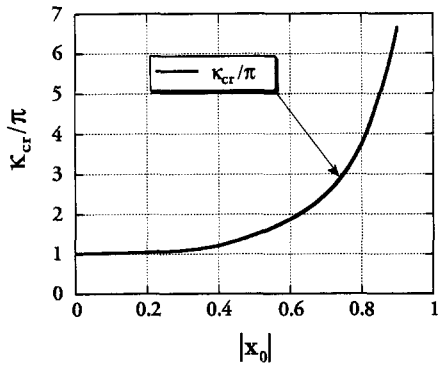

Fig. 4. The variation of the critical values of the wave number κ_{cr}, as a function of $|x_0|$.

discrepancies between different ranks were observed, leading to sufficiently accurate results at rank $M = 11$. The values of b_m as evaluated at rank $M = 11$ were eventually used for presenting the results.

When the layer's extension in the z and y directions is finite, as in the case presented in Fig. 1, the corresponding values of $\kappa_z = n\pi/H$ and $\kappa_y = l\pi/W$ replace the wave numbers in the z and y directions, respectively. Then for convective rolls having axes parallel to the shorter dimension (i.e. y) the eigenfunctions were evaluated and can be expressed in the form

$$T' = A_n \cos\left(\frac{n\pi z}{H}\right) \sum_{m=1}^{M} b_m \sin(m\pi x)$$

$$u' = -A_n \cos\left(\frac{n\pi z}{H}\right) \times \sum_{m=1}^{M} b_m \left(m^2 + \frac{n^2}{H^2}\right)\pi^2 \sin(m\pi x) \quad (18)$$

$$v' = 0$$

$$w' = \frac{A_n H}{n\pi} \sin\left(\frac{n\pi z}{H}\right) \times \sum_{m=1}^{M} b_m \left(m^2 + \frac{n^2}{H^2}\right) m\pi^3 \cos(m\pi x). \quad (19)$$

As $v' = 0$, a stream function can be used for presenting the results graphically. The complete solution for the temperature in terms of isotherms of $T = T_b + T'$ and for the flow field in terms of a stream function ψ, is presented in the form

$$\psi = -\frac{A_n H}{n\pi} \sin\left(\frac{n\pi z}{H}\right) \sum_{m=1}^{M} b_m \left(m^2 + \frac{n^2}{H^2}\right)\pi^2 \sin(m\pi x) \quad (20)$$

$$T = x + A_n \cos\left(\frac{n\pi z}{H}\right) \sum_{m=1}^{M} b_m \sin(m\pi x). \quad (21)$$

The results for the convective flow field are presented graphically in Figs. 5–7 for different values of $|x_0|$. The results as presented in Figs. 5–7, correspond to a value of $A_m = 0.2$ and to an aspect ratio $H = 4\pi/\kappa_{cr}$ which allows an integer value of $n = 4$ at the critical value of κ, corresponding to the respective value of $|x_0|$. From Fig. 5 it can be observed that the effect of the location of the axis of rotation within the porous box is definitely felt. Keeping in mind that, to the right of the rotation axis the centrifugal acceleration has a destabilizing effect, while to its left a stabilizing effect is expected, the results presented in Fig. 5b,c reaffirm this expectation, showing an eccentric shift of the convection cells towards the right side of the rotation axis. When the axis of rotation is moved further towards the hot wall, say at $|x_0| = 0.6$, as presented in Fig. 6a, weak convection cells appear even to the left of the rotation axis. This weak convection becomes stronger as $|x_0|$ increases, as observed in Figure 6b for $|x_0| = 0.7$. In Fig. 6b one can observe the formation of boundary layers associated with the primary convection cells to the right of the rotation axis. These boundary layers become more significant for $|x_0| = 0.8$, as represented by sharp stream lines gradients in Fig. 7a. When $|x_0| = 0.9$, as presented in Fig. 7b, the boundary layers of the primary convection are well established and the whole domain is filled with weaker secondary, tertiary and further convection cells. The results for the isotherms corresponding to values of $|x_0| = 0.$, 0.5, 0.6 and 0.7 are presented in Fig. 8. The amplitude of the temperature perturbations used in Fig. 8a was $A_n = 0.2$, in Fig. 8b $A_n = 0.1$ in Fig. 8c $A_n = 0.08$ and in Fig. 8d $A_n = 0.03$.

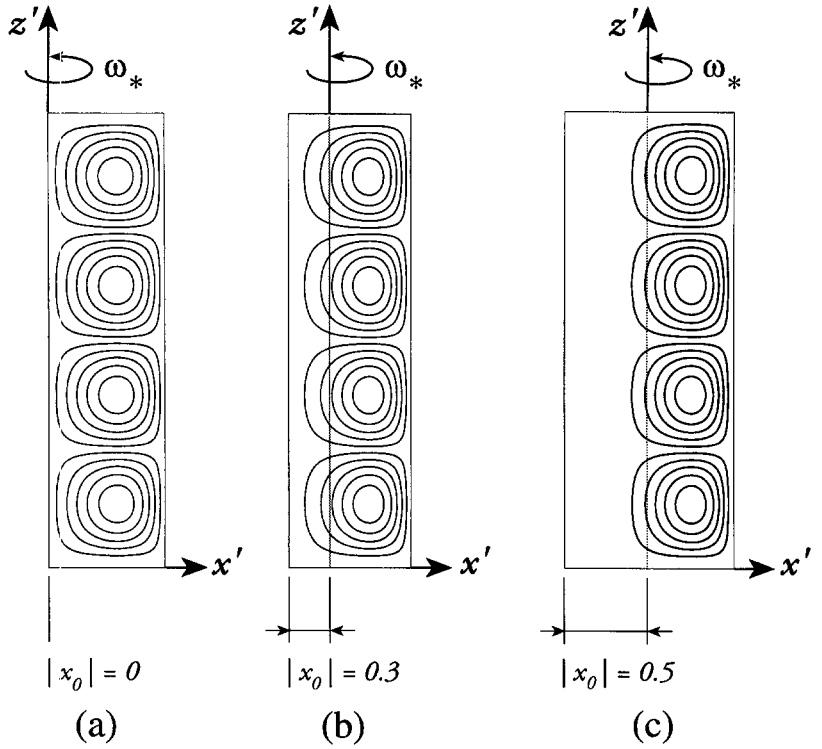

Fig. 5. The convective flow field at marginal stability for three different values of $|x_0|$; 10 stream lines equally divided between ψ_{min} and ψ_{max}. (a) At $|x_0| = 0$: $\psi_{min} = -1.378$; $\psi_{max} = 1.378$, (b) at $|x_0| = 0.3$; $\psi_{min} = -1.586$; $\psi_{max} = 1.586$ and (c) at $|x_0| = 0.5$: $\psi_{min} = -2.797$; $\psi_{max} = 2.797$.

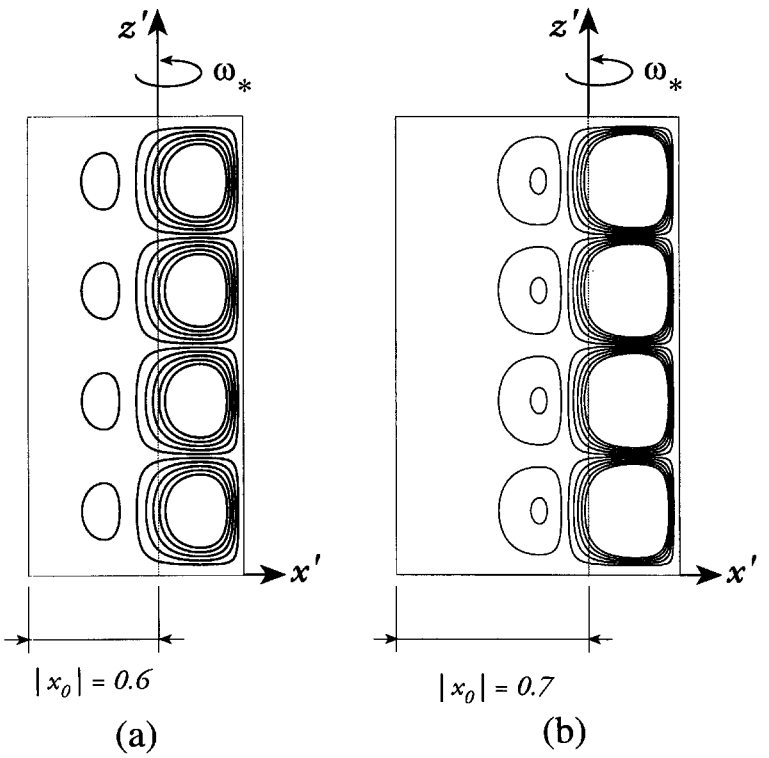

Fig. 6. The convective flow field at marginal stability for two different values of $|x_0|$; 10 stream lines equally divided between ψ_{min} and ψ_{max}. (a) At $|x_0| = 0.6$: $\psi_{min} = -2.808$; $\psi_{max} = 2.808$, and (b) at $|x_0| = 0.7$: $\psi_{min} = -2.666$; $\psi_{max} = 2.666$.

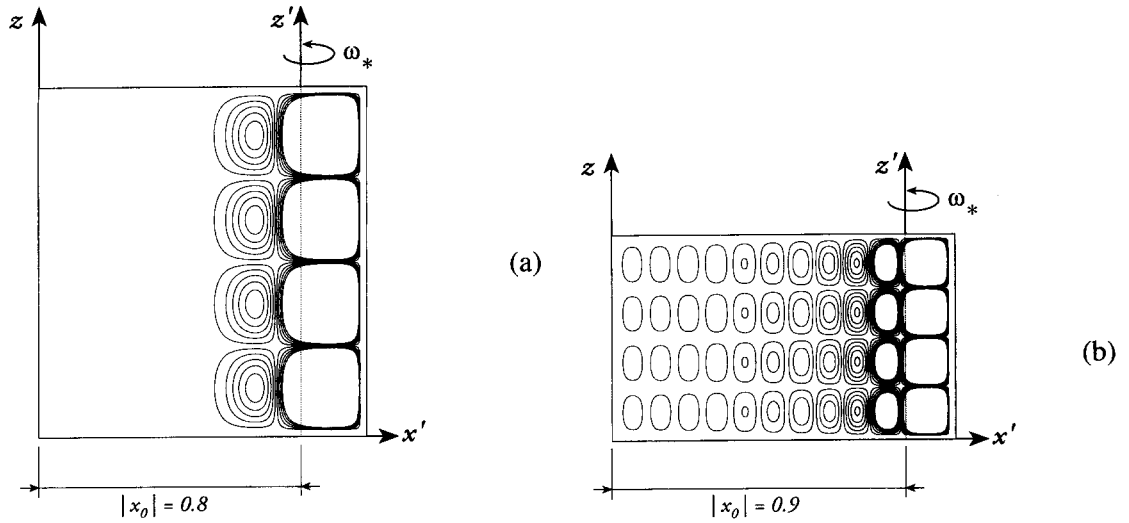

Fig. 7. The convective flow field at marginal stability for two different values of $|x_0|$; 10 stream lines equally divided between ψ_{min} and ψ_{max}. (a) At $|x_0| = 0.8$: $\psi_{min} = -2.609$; $\psi_{max} = 2.609$, and (b) at $|x_0| = 0.9$: $\psi_{min} = -19.317$; $\psi_{max} = 19.317$.

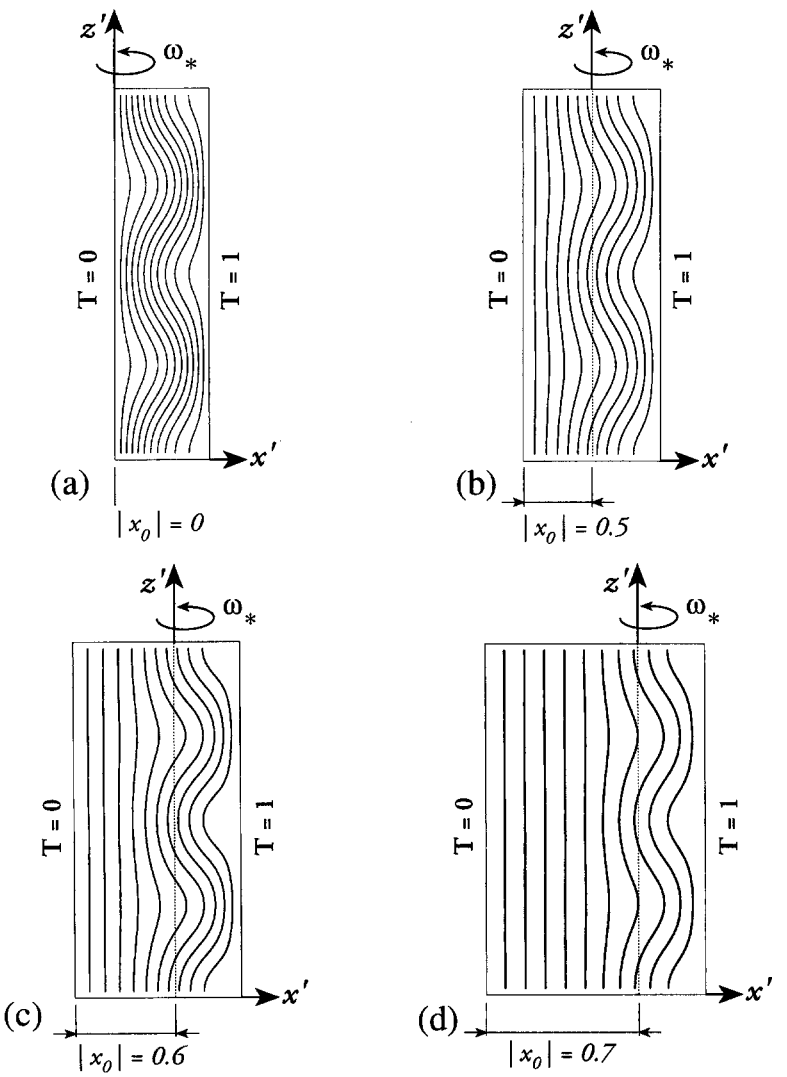

Fig. 8. The convective temperature field at marginal stability for four different values of $|x_0|$; 10 isotherms equally divided between $T_{min} = 0$ and $T_{max} = 1$.

The effect of moving the axis of rotation within the porous box on the temperature field is evident from Fig. 8.

5. CONCLUSIONS

The effect of the location of the axis of rotation on the convection and stability in a rotating porous layer subject to a centrifugal body force, was investigated analytically for the case when the rotation axis is placed within the boundaries of the domain. As a result, an alternating direction of the centrifugal body force is obtained leading to a stabilizing effect in the part of the domain located to the left of the rotation axis, and a destabilizing effect to its right. Significantly higher critical values of the centrifugal Rayleigh number and higher values of the critical wavenumber result as the value of $|x_0|$ increases. The convection is affected significantly by the variation in the value of $|x_0|$.

Acknowledgement—The author would like to thank the Foundation for Research Development for partially funding this research through the Core Programme Rolling Grant.

REFERENCES

1. P. Vadasz, Three-dimensional free convection in a long rotating porous box, *J. Heat Transfer* **115,** 639–644 (1993).
2. P. Vadasz, Fluid flow through heterogeneous porous media in a rotating square channel, *Transport Porous Media* **12,** 43–54 (1993).
3. P. R. Patil and G. Vaidyanathan, On setting up of convection currents in a rotating porous medium under the influence of variable viscosity, *Int. J. Engng Sci.* **21,** 123–130 (1983).
4. J. J. Jou and J. S. Liaw, Transient thermal convection in a rotating porous medium confined between two rigid boundaries, *Int. Commun. Heat Mass Transfer* **14,** 147–153 (1987).
5. J. J. Jou and J. S. Liaw, Thermal convection in a porous medium subject to transient heating and rotation, *Int. J. Heat Mass Transfer* **30,** 208–211 (1987).
6. N. Rudraiah, I. S. Shivakumara and R. Friedrich, The effect of rotation on linear and non-linear double-diffusive convection in sparsely packed porous medium, *Int. J. Heat Mass Transfer* **29,** 1301–1317 (1986).
7. E. Palm and a. Tyvand, Thermal convection in a rotating porous layer, *J. Appl. Math. Phys.* (ZAMP) **35,** 122–123 (1984).
8. P. Vadasz, Stability of free convection in a narrow porous layer subject to rotation, *Int. Commun. Heat Mass Transfer* **21,** 881–890 (1994).
9. P. Vadasz, Stability of free convection in a rotating porous layer distant from the axis of rotation (submitted).
10. S. Wolfram, *Mathematica: A System for Doing Mathematics by Computer* (2nd Edn). Wolfram Research Inc., Addison-Wesley, Redwood City, CA (1991).